Forest Fire Risk Mapping using Geographic Information System (GIS) and Analytic Hierarchy Process (AHP) in Lumbini Province, NEPAL

Introduction

In terrestrial environments, fire serves as an ecological tool in vegetation evolution when managed carefully; however, it becomes destructive when uncontrolled (Odum & Barrett, 1971). Between 2001 and 2020, forest fires in Nepal resulted in the loss of 7.07 million tons of biomass and 71 human casualties (Bhujel et al., 2022).

The unpredictable nature of forest fires and their increasing destructive impact (Artés et al., 2017) necessitate the identification of high-risk forest fire areas prior to fire incidents. Such proactive identification enables authorities to prevent, minimize, or control fire risks and develop adaptive strategies for effective response when fires occur (Chuvieco & Salas, 1996).

Geospatial technologies provide essential spatial and temporal information for timely and accurate analysis of complex fire models (Modugno et al., 2016; Vallejo-Villalta et al., 2019). Multi-Criteria Decision Analysis (MCDA) techniques facilitate decision-making in situations involving conflicting criteria and multiple options (Greco et al., 2016). Among MCDA methodologies, the Analytic Hierarchy Process (AHP) has gained widespread recognition in forest fire risk analysis (Busico et al., 2019; Gheshlaghi et al., 2020; Kayet et al., 2020).

Previous studies in Nepal have focused on specific regions: Parajuli et al. (2020) and Dhakal et al. (2024) developed spatial forest fire risk maps for the TAL-ChAL regions and Chure Terai Madhesh Landscape (CTML), respectively. However, these studies do not provide comprehensive coverage for Lumbini Province. This study addresses this research gap by developing a comprehensive forest fire risk map for Lumbini Province using GIS-based AHP methodology. The findings will support evidence-based decision-making for forest fire risk mitigation strategies in the province.

Study Area

The study area encompasses Lumbini Province, the third largest province by area in Nepal. The province exhibits significant multi-altitudinal variation, with regional landscapes stretching from high mountains in the north, through hills in the middle, to plains in the south. Forest ecosystems cover approximately 50% (974,000 hectares) of the province's total area, highlighting its ecological significance.

Lumbini Province contains three protected areas: Bardiya and Banke National Parks located in the Terai lowland region, and Dhorpatan Hunting Reserve situated in the hilly and mountainous region (MOFE, 2020). The province experiences a humid subtropical climate characterized by four distinct seasons: winter (January-February), summer (March-May), monsoon (June-September), and post-monsoon (October-December) (DHM, 2020).

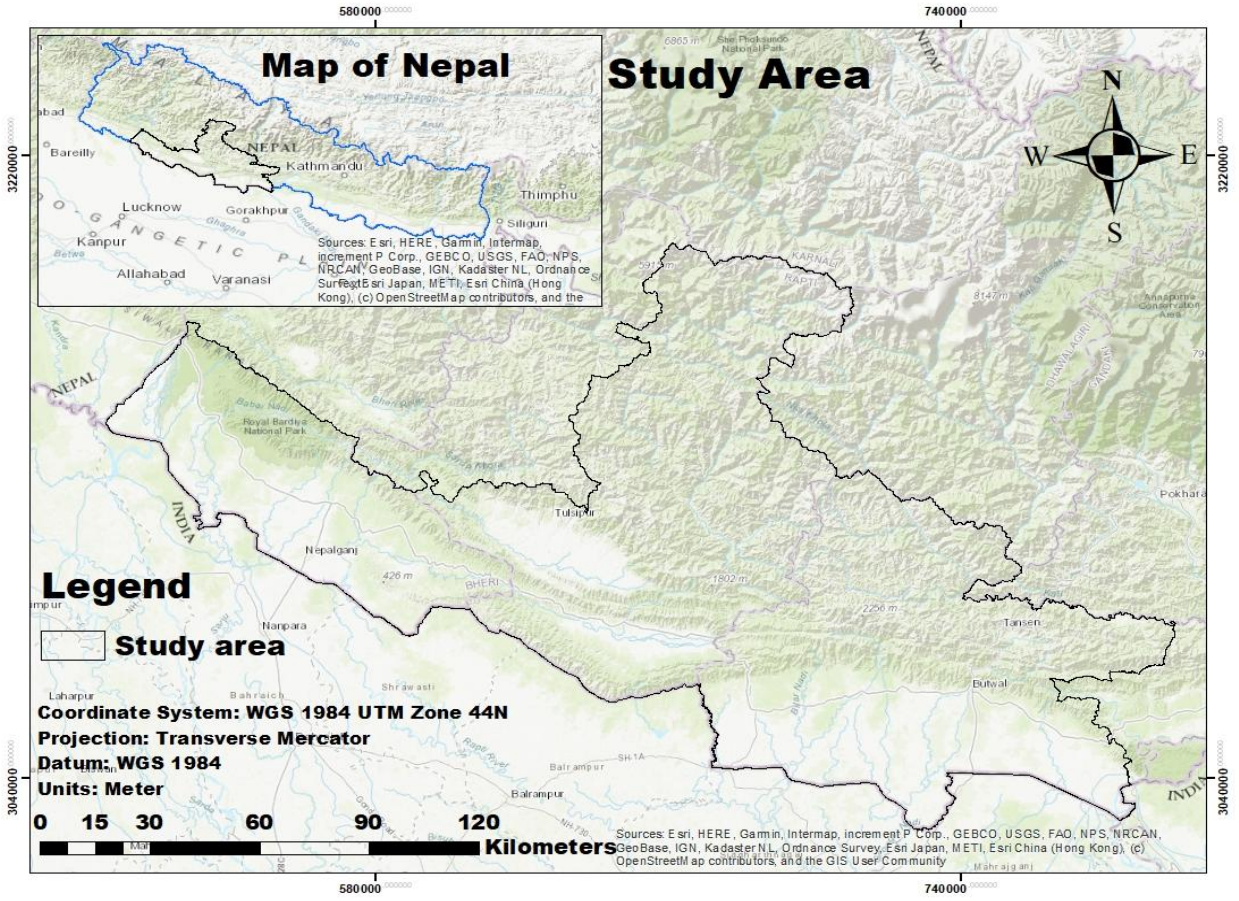

Fig 1: Study area

Methodology

Datasets Used

Table 1: Remote Sensing and GIS Datasets

Factors	Sources	Data Format	Resolution	Data Period
Land Cover	ICIMOD - International Centre for Integrated Mountain Development	Raster	30 m	2022
NDVI	Landsat 8 OLI-TIRS (https://earthexplorer.usgs.gov/)	Raster	30 m	2024
Slope Elevation Aspect	SRTM DEM (https://earthexplorer.usgs.gov/)	Raster	30 m	2014
TWI				
Distance from Settlement Distance from Road	Humanitarian Data Exchange	Vector	1:25000	2015 2025
Precipitation	CHIRPS Daily: Climate Hazards Center InfraRed Precipitation With Station Data	Raster	5.5 km	2000-2025
LST	MOD11A1.061 Terra Land Surface Temperature and Emissivity Daily Global 1km	Raster	1 km	2000-2025
Wind Speed	Global Wind Atlas (Global Wind Atlas)	Raster	250 m	2020
VIIRS hotspot	Fire Information for Resource Management System (NASA | LANCE | FIRMS)	Vector	375 m	2024-2025

NDVI, LST, and precipitation data were processed using Python's Google Earth Engine API, while remaining factors were analyzed in ArcMap 10.8. All datasets were resampled to 30m resolution and categorized according to Table 2. Forest fire risk mapping was conducted through linear weighted combination of thematic layers using corresponding AHP weights. The resulting risk

map was validated using ROC curve analysis with fire incidents having nominal and high confidence levels. Figure 2 illustrates the complete methodological framework.

Causative Factors

1. **LC**: Dense and dry vegetation in close proximity increases forest fire susceptibility and facilitates rapid fire spread (Erten et al., 2005; Veena et al., 2017).
2. **NDVI:** NDVI values indicate vegetation density and moisture content, which directly influence forest fire risk susceptibility (Li et al., 2021; Saloum & Abdou, 2016).
3. **Slope:** Steeper slopes accelerate fire spread by facilitating fuel preheating and enhancing upward fire propagation through increased wind speeds (Estes et al., 2017; Ajin et al., 2017).
4. **Aspect:** Slope aspect determines microclimate conditions including solar radiation, temperature, and moisture content, which collectively influence fire risk (Jaafari & Pourghasemi, 2019; Zhang et al., 2022).
5. **Elevation:** Higher elevations experience reduced fire occurrence due to increased rainfall, lower temperatures, and higher humidity compared to lower elevations (Falkowski et al., 2005; Chuvieco & Congalton, 1989).
6. **TWI:** Higher Topographic Wetness Index values indicate greater soil moisture content, resulting in reduced forest fire risk (Adab et al., 2013a; Al-Fugara et al., 2021).
7. **Distance from Settlement:** Proximity to human settlements increases forest fire risk through both intentional and accidental fire ignition from anthropogenic activities (Jaafari et al., 2018; Geng et al., 2020).
8. **Distance from Road Roads:** increase fire risk as pedestrians and vehicles can initiate fires either purposefully or accidentally (Veena et al., 2017; Ricotta et al., 2018).
9. **Precipitation:** Lower precipitation reduces fuel moisture content, thereby increasing forest fire probability (Abedi Gheshlaghi, 2019; Mondal & Sukumar, 2016).
10. **LST:** Higher land surface temperatures increase evapotranspiration rates, creating dry fuel conditions that elevate forest fire risk (Bonora et al., 2013; Flannigan et al., 2016).
11. **Wind Speed:** Wind speed accelerates fire ignition and spread by supplying oxygen and reducing fuel moisture content (Kanga et al., 2017; Karafyllidis & Thanailakis, 1997).

Methodological Framework

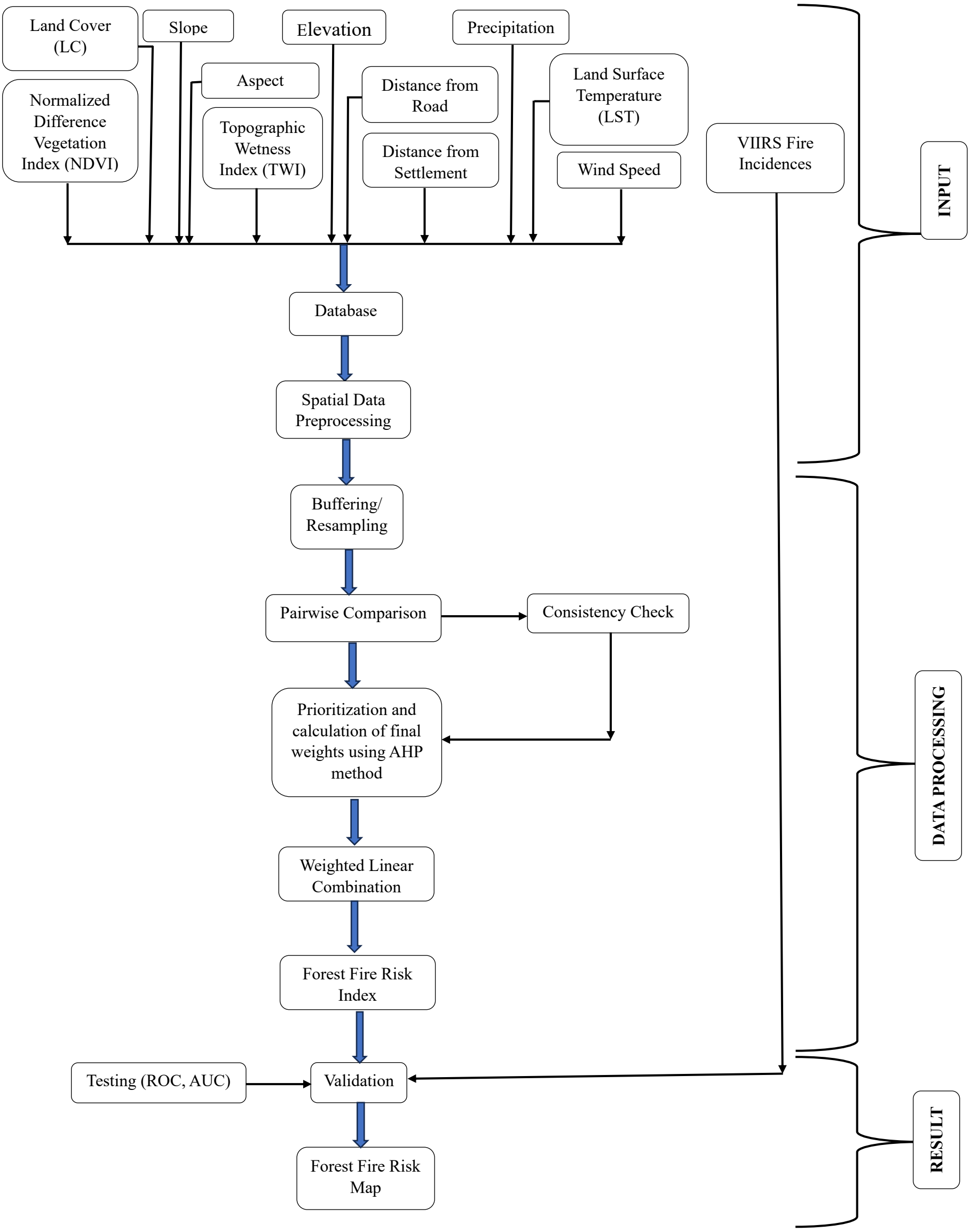

Fig. 2: Methodological framework of the study

Assignment of weightage to the parameters

The AHP approach facilitates decision-making in complex multi-criteria problems by enabling systematic prioritization of alternatives (Saaty, 1980). Weight assignment to thematic layers is crucial for forest fire zone prediction as model outputs depend significantly on weight selection. Relative priority values were assigned to each criterion based on causative factor understanding, historical fire patterns, study area characteristics, and comprehensive literature review.

The AHP methodology involved pairwise comparison (Table 4) of all elements using importance scales (Table 2) for forest fire probability assessment. Detailed AHP procedures are documented in Nikhil et al. (2021) and Tiwari et al. (2021). To ensure consistency and avoid conflicting judgments from multiple decision-makers, a single decision-maker conducted all pairwise comparisons.

Table 1. Saaty's Scale for Decision-Making (Saaty, 1980)

Level of importance	**Definition**
1	Equivalent importance to the objective
3	Considerable importance of one over another
5	Significant importance
7	Paramount importance
9	Imperative importance
4,6,8	Mid-range values
Reciprocals	Utilize for inverse comparison

Table 3: Random Inconsistency values

Number of criteria	1	2	3	4	5	6	7	8	9	10	11
Random Inconsistency	**0**	0	0.58	0.9	1.12	1.24	1.32	1.41	1.45	1.49	1.51

Comparison consistency was evaluated using the consistency ratio (CR) through Eq. 5, with CR values below 0.1 indicating reliable weights (Saaty, 1980). The validated weights were subsequently applied to thematic layers for forest fire risk mapping, ensuring accurate and consistent determination of each criterion's relative importance.

The consistency index (CI) was calculated using Eq.4 as follows:

$\mathrm{CI} = \frac{(\lambda \mathrm{max} - \mathrm{n})}{(\mathrm{n}-1)}$ ... ... (4) Where n is the number of factors used.

The consistency ratio (CR) was calculated using Eq.5 as follows:

$\mathrm{CR} = \frac{\mathrm{CI}}{\mathrm{RI}}$ ... ... (5) Where RI is the random index (Table 3).

Table 4: Pairwise Comparison

Factors	LC	LST	Ele	Ppt	DR	TWI	DS	Sl	As	NDVI	WS
LC	1	3	2	3	2	4	2	3	3	2	5
LST	1/3	1	1/2	3	1/3	4	1/2	2	2	1/3	4
Ele	1/2	2	1	3	1/3	4	2	2	3	1/2	5
Ppt	1/3	1/3	1/3	1	1/4	2	1/4	1/2	1/2	1/4	3
DR	0.5	3	3	4	1	5	2	2	3	1/2	5
TWI	1/4	0.25	0.25	1/2	1/5	1	1/4	1/3	1/3	1/4	2
DS	1/2	2	1/2	4	1/2	4	1	3	3	1/2	4
Sl	1/3	1/2	1/2	2	1/2	3	1/3	1	2	1/2	4
As	1/3	1/2	1/3	2	1/3	3	1/3	1/2	1	1/3	4
NDVI	1/2	3	2	4	2	4	2	2	3	1	6
WS	1/5	1/4	1/5	1/3	1/5	1/2	1/4	1/4	1/4	1/6	1

Table 5: Normalized pairwise comparison matrix and computation of weights

Factors	LC	LST	Ele	Ppt	DR	TWI	DS	Sl	As	NDVI	WS	Criteria Weights
LC	0.21	0.19	0.19	0.11	0.26	0.12	0.18	0.18	0.14	0.32	0.12	0.18
LST	0.07	0.06	0.05	0.11	0.04	0.12	0.05	0.12	0.09	0.05	0.09	0.08
Ele	0.10	0.13	0.09	0.11	0.04	0.12	0.18	0.12	0.14	0.08	0.12	0.11
Ppt	0.07	0.02	0.03	0.04	0.03	0.06	0.02	0.03	0.02	0.04	0.07	0.04
DR	0.10	0.19	0.28	0.15	0.13	0.14	0.18	0.12	0.14	0.08	0.12	0.15
TWI	0.05	0.02	0.02	0.02	0.03	0.03	0.02	0.02	0.02	0.04	0.05	0.03
DS	0.10	0.13	0.05	0.15	0.07	0.12	0.09	0.18	0.14	0.08	0.09	0.11
Sl	0.07	0.03	0.05	0.07	0.07	0.09	0.03	0.06	0.09	0.08	0.09	0.07
As	0.07	0.03	0.03	0.07	0.04	0.09	0.03	0.03	0.05	0.05	0.09	0.05
NDVI	0.10	0.19	0.19	0.15	0.26	0.12	0.18	0.12	0.14	0.16	0.14	0.16
WS	0.04	0.02	0.02	0.01	0.03	0.01	0.02	0.02	0.01	0.03	0.02	0.02
						L_{max} = 11.67						
						n = 11						
						CI = 0.07						
						RI = 1.51						
						CR = 0.04						

For both Tables 4 and 5: LC=Land Cover, NDVI=Normalized Difference Vegetation Index, Sl=Slope, As=Aspect, El=Elevation, TWI=Topographic Wetness Index, DS=Distance from Settlement, DR=Distance from Road, Ppt=Precipitation, LST=Land Surface Temperature, WS=Windspeed

Saaty (1980) recommends a CR value below 0.1 to ensure reliable pairwise comparisons. The calculated consistency ratio of 0.04 confirms the reliability of the pairwise comparison matrix (Table 4) and validates the FFRI model.

Causative Factors

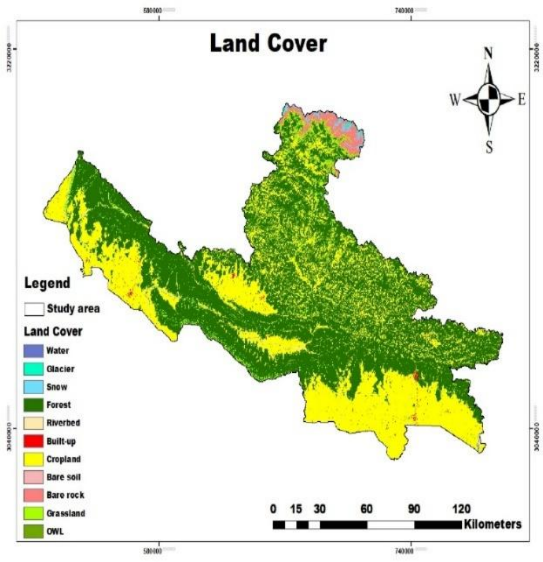

Fig 3: Land Cover

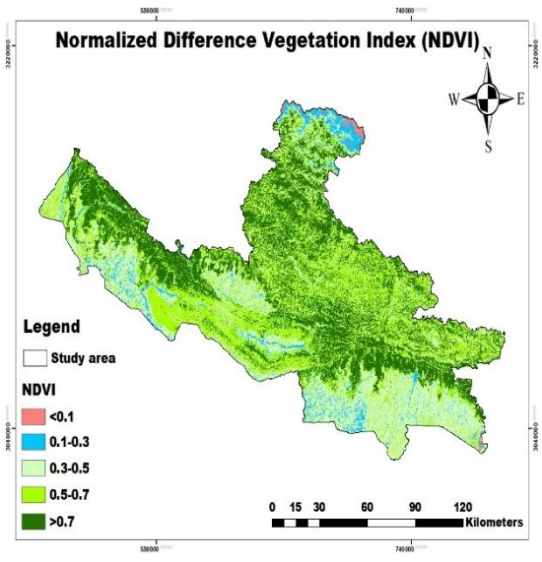

Fig 4: NDVI

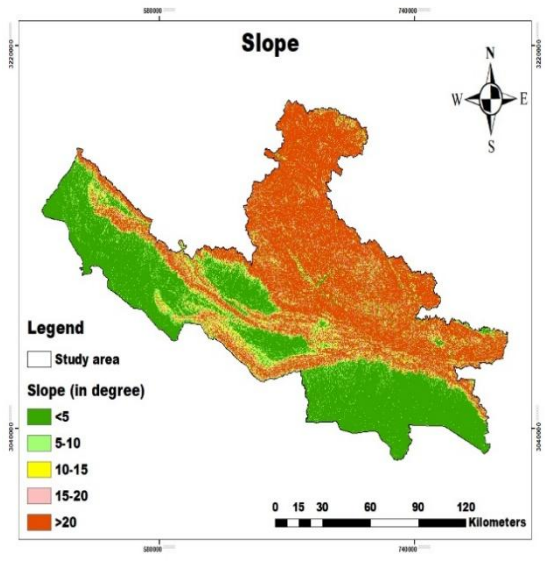

Fig 5: Slope

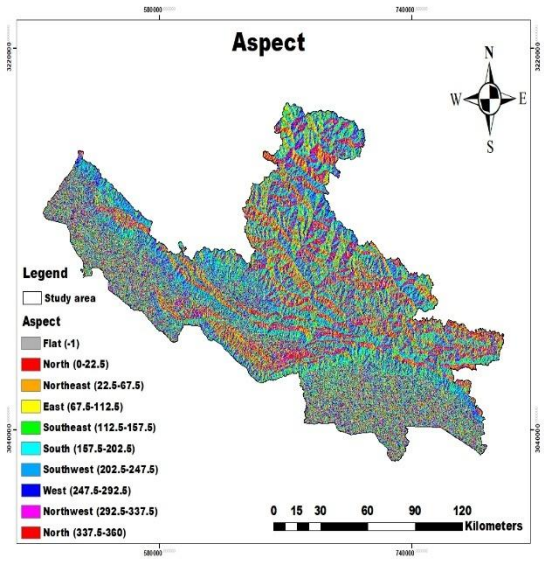

Fig 6: Aspect

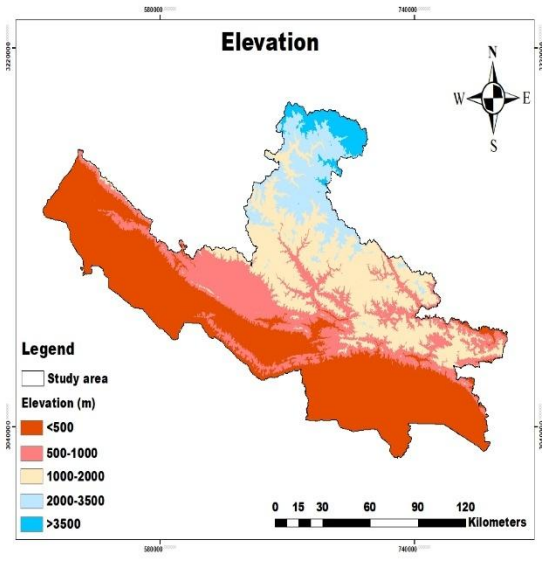

Fig 7: Elevation

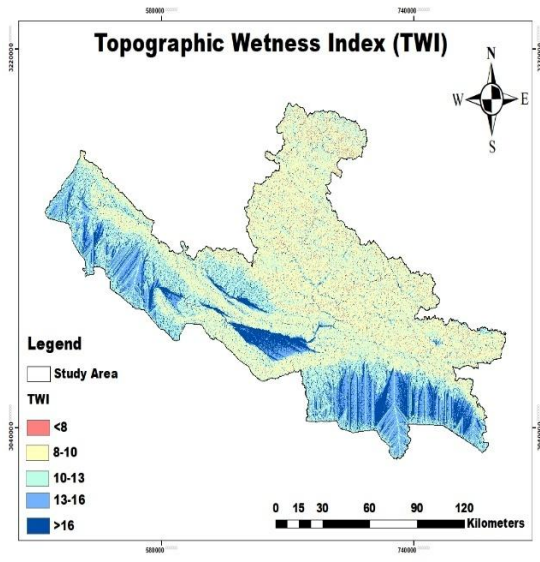

Fig 8: TWI

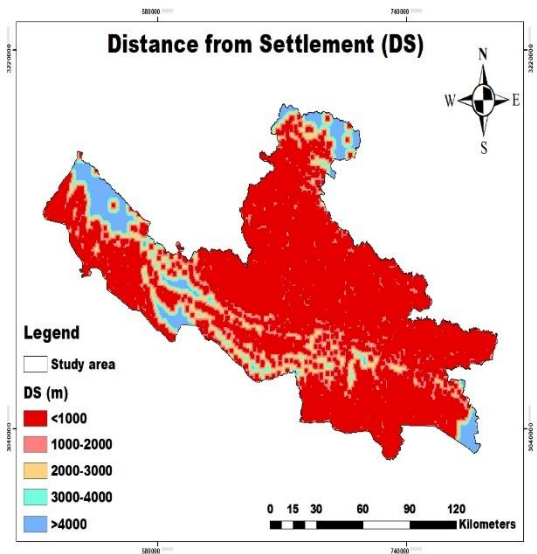

Fig 9: Distance from Settlement

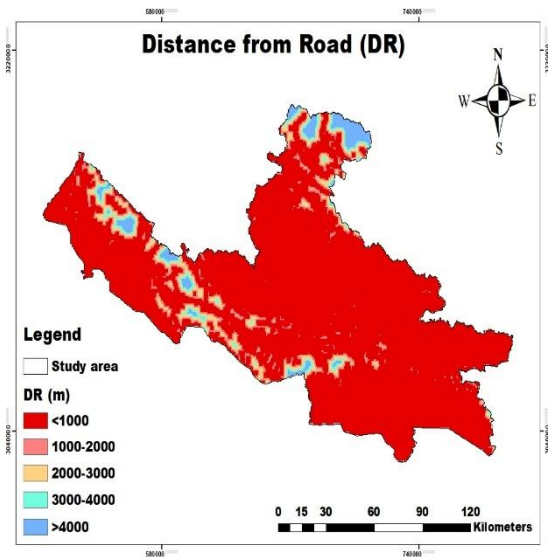

Fig 10: Distance from

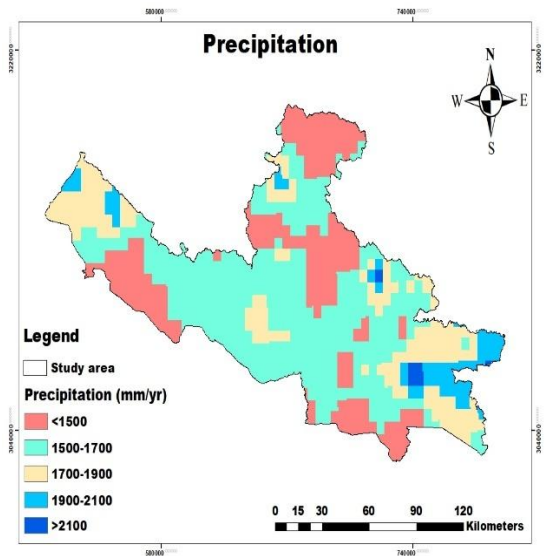

Fig 11: Precipitation

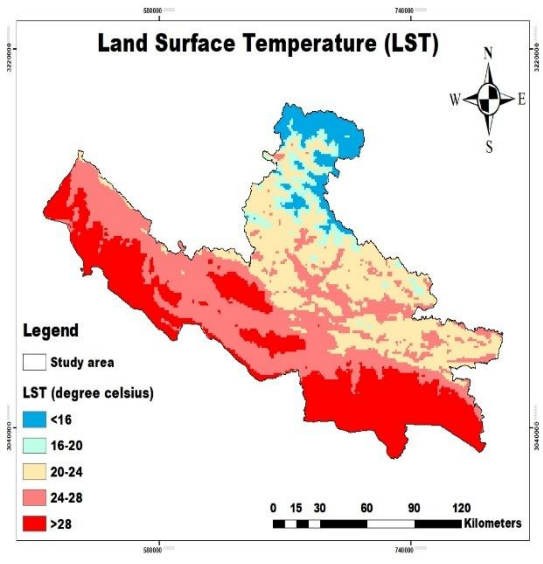

Fig 12: Land Surface Temperature

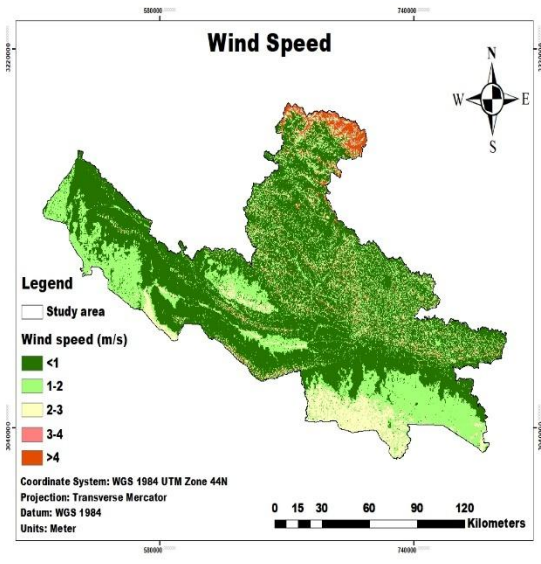

Fig 13: Wind Speed

Preparation of forest fire risk map

Forest fire risk zones were generated in ArcMap 10.8 using weighted linear combination, where individual thematic layer weights were multiplied by their respective component weights and summed to calculate the Forest Fire Risk Index (FFRI) according to Eq. 3.

FFRI = 0.18 * LC + 0.16 * NDVI + 0.07 * S + 0.05 * A + 0.11 * E + 0.03 * TWI + 0.11 * DS + 0.15 * DR + 0.04 * P + 0.08 * LST + 0.02 * WS…… (3)

Where FFRI = Forest Fire Risk Index, LC = Land Cover, NDVI = Normalized Difference Vegetation Index, S = Slope, A = Aspect, E = Elevation, TWI = Topographic Wetness Index, DS = Distance from Settlement, DR = Distance from Road, P = Precipitation, LST = Land Surface Temperature, and WS = Wind Speed

Validation of the map

Model validation is essential for assessing forest fire vulnerability prediction efficacy (Jaafari et al., 2017; Pham et al., 2020). The ROC-AUC curve, a widely used method for evaluating modeling effectiveness, was employed to validate the generated forest fire risk map (Adab et al., 2013b; Ghorbanzadeh & Blaschke, 2018).

Result

The computed weights for each factor using the AHP method and the potentiality of forest fire risk in different classes of each factor are presented in Table 6.

Table 6: Weights and ratings assigned to factors and classes for forest fire risk modeling

S. No	Factors	Class	Potentiality for FFRM	Rating	AHP Weight
1	Land Cover	Forest	Very High	5	0.18
		Grassland	High	4	
		Other Wooded Land (OWL)	Medium	3	
		Cropland	Low	2	
		Water, Snow, Glacier, Riverbed, Built-up, Bare soil, Bare rock	Very Low	1	
2	NDVI	>0.7	Very High	5	0.16
		0.5-0.7	High	4	
		0.3-0.5	Moderate	3	
		0.1-0.3	Low	2	
		<0.1	Very Low	1	
3	Slope (degree)	>20	Very High	5	0.07
		15-20	High	4	
		10-15	Moderate	3	
		5-10	Low	2	
		<5	Very Low	1	
4	Aspect	South/South West	Very High	5	0.05
		South East	High	4	
		East/West	Moderate	3	
		North East/North West	Low	2	
		Flat/North	Very Low	1	
5	Elevation (m)	<500	Very High	5	0.11
		500-1000	High	4	
		1000-2000	Moderate	3	
		2000-3500	Low	2	
		>3500	Very Low	1	
6	TWI	<8	Very High	5	0.03
		8-10	High	4	
		10-13	Moderate	3	
		13-16	Low	2	
		>16	Very Low	1	

7	Distance from Settlement (m)	<1000	Very High	5	0.11
		1000-2000	High	4	
		2000-3000	Moderate	3	
		3000-4000	Low	2	
		>4000	Very Low	1	
8	Distance from Road (m)	<1000	Very High	5	0.15
		1000-2000	High	4	
		2000-3000	Moderate	3	
		3000-4000	Low	2	
		>4000	Very Low	1	
9	Precipitation (mm)	<1500	Very High	5	0.04
		1500-1700	High	4	
		1700-1900	Moderate	3	
		1900-2100	Low	2	
		>2100	Very Low	1	
10	LST (°c)	>28	Very High	5	0.08
		24-28	High	4	
		20-24	Moderate	3	
		16-20	Low	2	
		<16	Very Low	1	
11	Wind Speed (m/s)	<4	Very High	5	0.02
		3-4	High	4	
		2-3	Moderate	3	
		1-2	Low	2	
		>1	Very Low	1	

Fire Risk Map

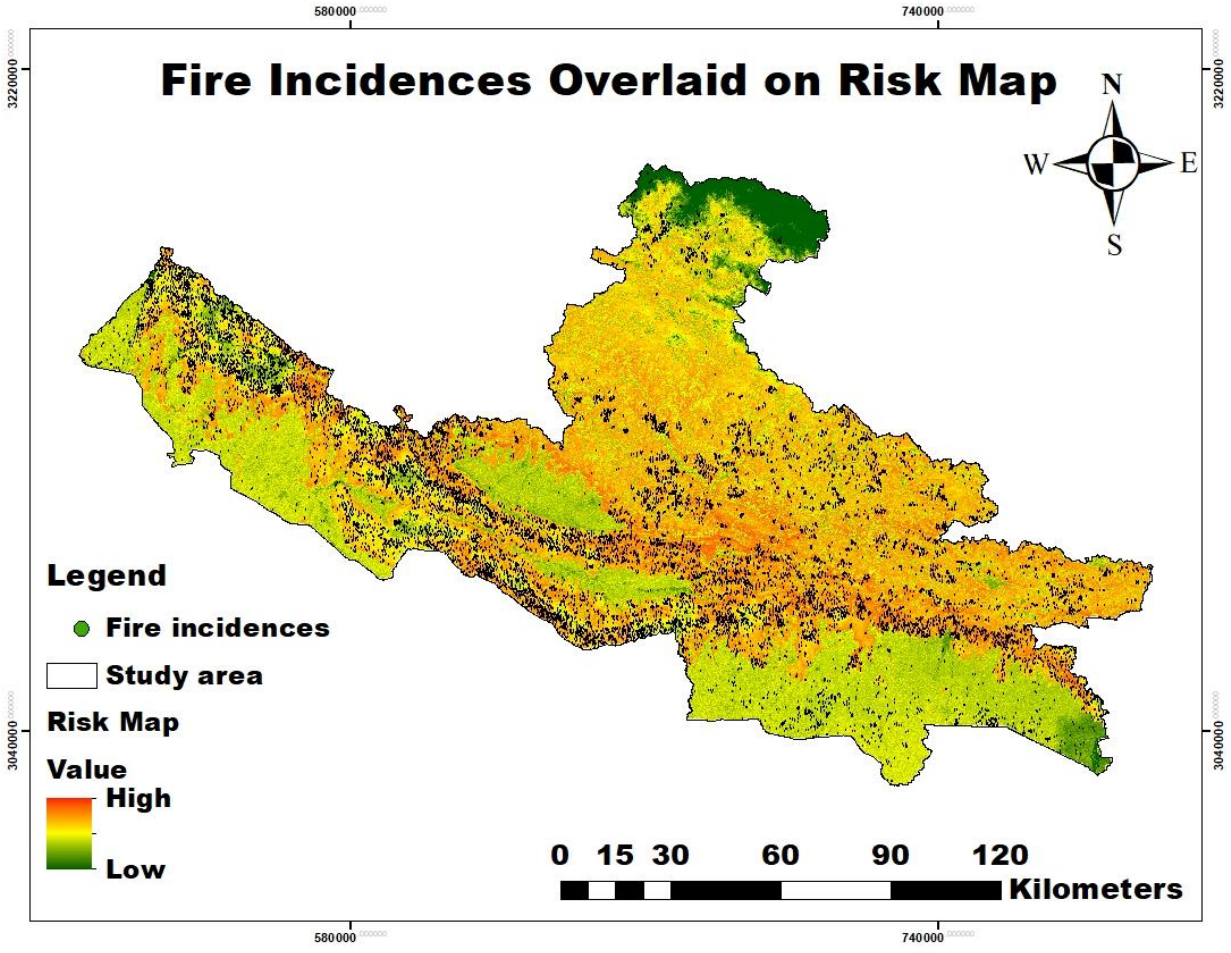

Fig 14: Fire incidences overlaid on risk map

A total of 14,516 fire incidents with confidence levels nominal and high occurred between 2024 and 2025 and were overlaid on the risk map (Fig. 14). Fire risk was classified into five categories: very low, low, medium, high, and very high risk (Fig. 15), with area coverage shown in Fig. 16. District-wise risk distribution is presented in Fig. 17, while Fig. 18 displays the ROC curve for model validation.

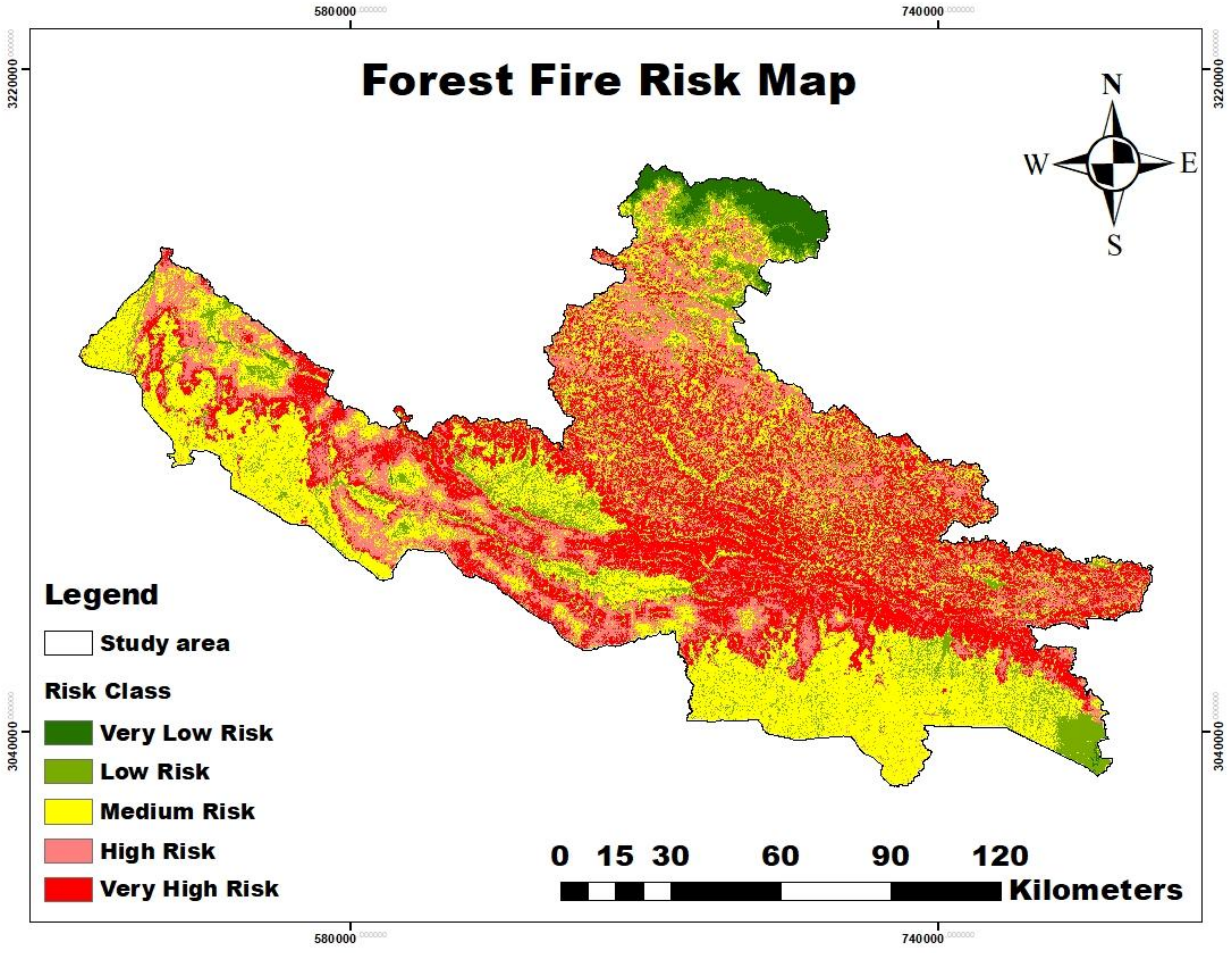

Fig 15: Forest Fire Risk Map

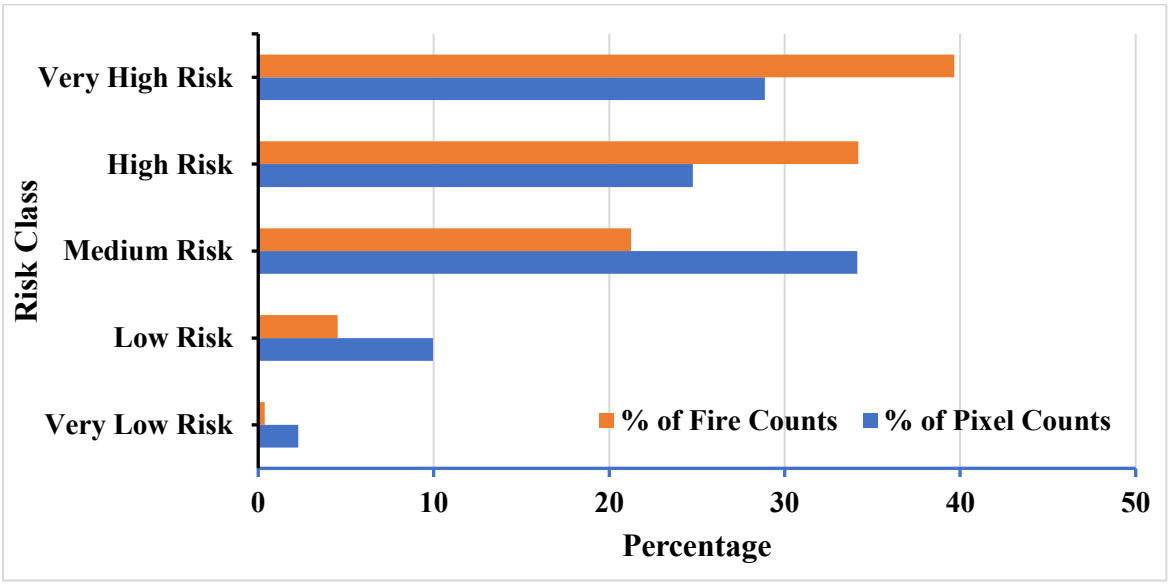

Fig 16: Percentage of pixel and fire counts in different classes

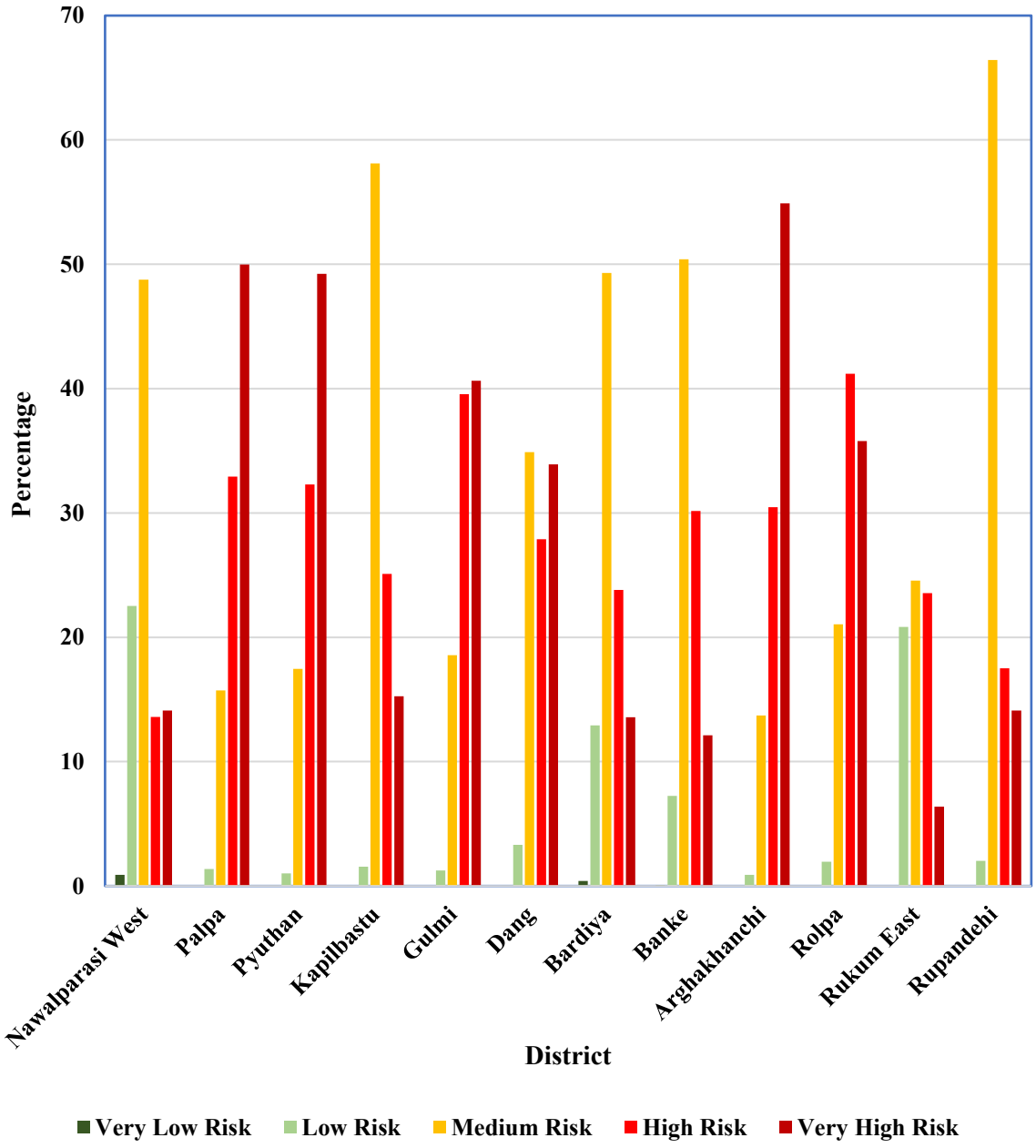

Fig 17: Distribution of risk classes in different districts

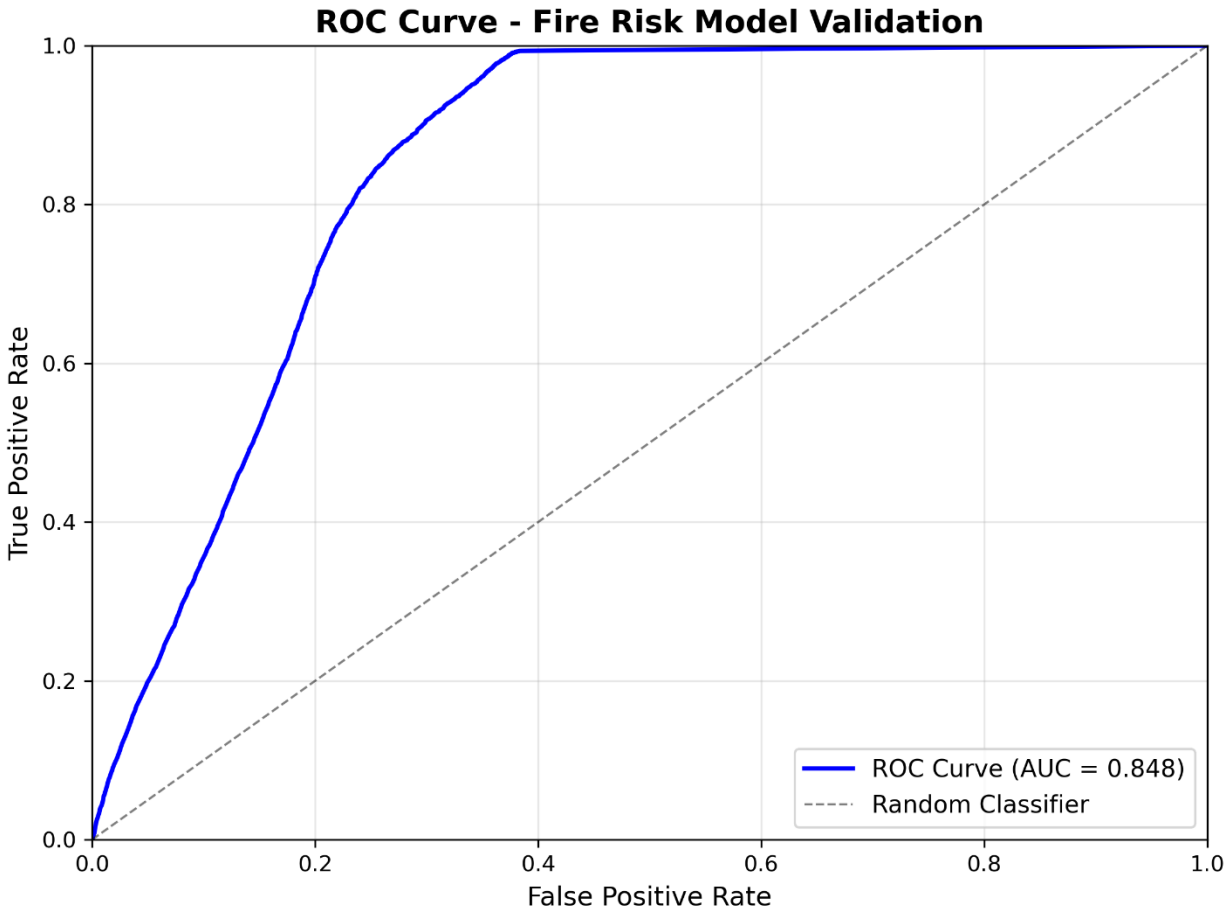

Fig 18: ROC curve

Conclusion

This study successfully developed a comprehensive forest fire risk assessment for Lumbini Province, Nepal's topographically diverse region, using integrated remote sensing data, GIS, and AHP methodology. The consistency ratio of 0.04 validates the reliability of pairwise comparisons among causative factors, with NDVI receiving the highest weightage, followed by anthropogenic factors (distance from settlements and roads).

The generated forest fire risk map achieved an AUC value of 0.848, demonstrating high reliability and providing a robust decision-support tool for local government agencies, forest managers, and community stakeholders in forest fire management and ecosystem resilience enhancement. The spatial analysis revealed that Palpa, Pyuthan, and Arghakhanchi districts contain the highest fire risk areas, requiring prioritized attention for fire prevention and management strategies.

This research demonstrates the efficacy of integrating GIS-based multi-criteria decision analysis for forest fire risk assessment in Nepal's complex terrain. However, several limitations warrant consideration for future research. Enhanced methodological approaches could incorporate additional fire causation factors, integrate expert opinions from local forest managers, and employ alternative multi-criteria decision analysis techniques. Furthermore, incorporating multi-temporal analysis, multi-source remote sensing data with varying spatial resolutions, and comprehensive ground-truth validation would significantly strengthen model credibility and robustness.

The findings provide a foundation for evidence-based fire management policies and can guide resource allocation for fire prevention infrastructure in high-risk areas across Lumbini Province.

References

Abedi Gheshlaghi, H. (2019). Using GIS to Develop a Model for Forest Fire Risk Mapping. *Journal of the Indian Society of Remote Sensing*, *47*(7), 1173–1185. https://doi.org/10.1007/S12524-019-00981-Z

Adab, H., Kanniah, K. D., & Solaimani, K. (2013a). Modeling forest fire risk in the northeast of Iran using remote sensing and GIS techniques. *Natural Hazards*, *65*(3), 1723–1743. https://doi.org/10.1007/s11069-012-0450-8

Ajin, R. S., Loghin, A. M., Vinod, P. G., & Jacob, M. K. (2017). The risk analysis of potential forest fires in a wildlife sanctuary in the western ghats (Southwest Indian Peninsula) using geospatial techniques. *International Journal of Health System and Disaster Management*, *5*(1), 18-23.

Al-Fugara, A. K., Mabdeh, A. N., Ahmadlou, M., Pourghasemi, H. R., Al-Adamat, R., Pradhan, B., & Al-Shabeeb, A. R. (2021). Wildland fire susceptibility mapping using support vector regression and adaptive neuro-fuzzy inference system-based whale optimization algorithm and simulated annealing. *ISPRS International Journal of Geo-Information*, *10*(6), 382.

Artés, T., Cencerrado, A., Cortés, A., & Margalef, T. (2017). Time aware genetic algorithm for forest fire propagation prediction: exploiting multi-core platforms. *Concurrency and Computation: Practice and Experience*, *29*(9). https://doi.org/10.1002/CPE.3837

Bhujel, K. B., Sapkota, R. P., & Khadka, U. R. (2022). Temporal and spatial distribution of forest fires and their environmental and socio-economic implications in Nepal. *Journal of Forest and Livelihood*, *21*(1), 1-13.

Bonora, L., Conese, C. C., Marchi, E., Tesi, E., & Montorselli, N. B. (2013). Wildfire occurrence: Integrated model for risk analysis and operative suppression aspects management.

Busico, G., Giuditta, E., Kazakis, N., & Colombani, N. (2019). A hybrid GIS and AHP approach for modelling actual and future forest fire risk under climate change accounting water resources attenuation role. *Sustainability*, *11*(24), 7166.

Chuvieco, E., & Salas, J. (1996). Mapping the spatial distribution of forest fire danger using GIS. *International Journal of Geographical Information Science*, *10*(3), 333-345.

Department of Hydrology and Meteorology [DHM]. (2020). *Department of Hydrology and Meteorology*. Government of Nepal. https://dhm.gov.np

Dhakal, M., Bhatta, B., Lamichhane, P., & Parajuli, A. (2024). Synergistic approaches in forest fire risk mapping using fuzzy AHP and machine learning models in the Chure Tarai Madhesh Landscape (CTML) of Nepal. *Geomatics, Natural Hazards and Risk*, *15*(1). https://doi.org/10.1080/19475705.2024.2436540

Estes, B. L., Knapp, E. E., Skinner, C. N., Miller, J. D., & Preisler, H. K. (2017). Factors influencing fire severity under moderate burning conditions in the Klamath Mountains, northern California, USA. *Ecosphere*, *8*(5), e01794.

Erten, E., Kurgun, V., & Musaoglu, N. (2004, July). Forest fire risk zone mapping from satellite imagery and GIS: a case study. In *XXth Congress of the International Society for Photogrammetry and Remote Sensing, Istanbul, Turkey* (pp. 222-230).

Flannigan, M. D., Wotton, B. M., Marshall, G. A., De Groot, W. J., Johnston, J., Jurko, N., & Cantin, A. S. (2016). Fuel moisture sensitivity to temperature and precipitation: climate change implications. *Climatic Change*, *134*, 59-71.

Falkowski, M. J., Gessler, P. E., Morgan, P., Hudak, A. T., & Smith, A. M. (2005). Characterizing and mapping forest fire fuels using ASTER imagery and gradient modeling. *Forest ecology and management*, *217*(2-3), 129-146.

Geng, M. Y., Ma, K. X., Sun, Y. K., Wo, X. T., & Wang, K. (2020). Changes of land use/cover and landscape in Zhalong wetland as "red-crowned cranes country", Heilongjiang province, China. *Global NEST Journal*, *22*(4), 477-483.

Gheshlaghi, H. A., Feizizadeh, B., & Blaschke, T. (2020). GIS-based forest fire risk mapping using the analytical network process and fuzzy logic. *Journal of Environmental Planning and Management*, *63*(3), 481-499.

Ghorbanzadeh, O., & Blaschke, T. (2018, July). Wildfire susceptibility evaluation by integrating an analytical network process approach into GIS-based analyses. In *Proceedings of ISERD International Conference*.

Greco, S., Figueira, J., & Ehrgott, M. (2016). *Multiple criteria decision analysis* (Vol. 37). New York: springer.

Jaafari, A., Gholami, D. M., & Zenner, E. K. (2017). A Bayesian modeling of wildfire probability in the Zagros Mountains, Iran. *Ecological informatics*, *39*, 32-44.

Jaafari, A., & Pourghasemi, H. R. (2019). Factors influencing regional-scale wildfire probability in Iran: an application of random forest and support vector machine. In *Spatial modeling in GIS and R for Earth and environmental sciences* (pp. 607-619). Elsevier.

Jaafari, A., Zenner, E. K., & Pham, B. T. (2018). Wildfire spatial pattern analysis in the Zagros Mountains, Iran: A comparative study of decision tree based classifiers. *Ecological informatics*, *43*, 200-211.

Kanga, S., Tripathi, G., & Singh, S. K. (2017). Forest fire hazards vulnerability and risk assessment in Bhajji forest range of Himachal Pradesh (India): a geospatial approach. *Journal of Remote Sensing & GIS*, *8*(1), 1-16.

Karafyllidis, I., & Thanailakis, A. (1997). A model for predicting forest fire spreading using cellular automata. *Ecological Modelling*, *99*(1), 87-97.

Kayet, N., Chakrabarty, A., Pathak, K., Sahoo, S., Dutta, T., & Hatai, B. K. (2020). Comparative analysis of multi-criteria probabilistic FR and AHP models for forest fire risk (FFR) mapping in Melghat Tiger Reserve (MTR) forest. *Journal of forestry research*, *31*, 565-579.

Li, J., Zhao, Y., Zhang, A., Song, B., & Hill, R. L. (2021). Effect of grazing exclusion on nitrous oxide emissions during freeze-thaw cycles in a typical steppe of Inner Mongolia. *Agriculture, ecosystems & environment*, *307*, 107217.

Ministry of Forests and Environment [MOFE]. (2020). *Ministry of Forests and Environment*. Government of Nepal. https://mofe.gov.np

Modugno, S., Balzter, H., Cole, B., & Borrelli, P. (2016). Mapping regional patterns of large forest fires in Wildland–Urban Interface areas in Europe. *Journal of environmental management*, *172*, 112-126.

Mondal, N., & Sukumar, R. (2016). Fires in seasonally dry tropical forest: testing the varying constraints hypothesis across a regional rainfall gradient. *PloS one*, *11*(7), e0159691.

Nikhil, S., Danumah, J. H., Saha, S., Prasad, M. K., Rajaneesh, & A., Pratheesh, &, Mammen, C., Ajin, R. S., & Kuriakose, S. L. (2021). *Application of GIS and AHP Method in Forest Fire Risk Zone Mapping: a Study of the Parambikulam Tiger Reserve, Kerala, India*. https://doi.org/10.1007/s41651-021-00082-x/Published

Odum, E. P., & Barrett, G. W. (1971). *Fundamentals of ecology* (Vol. 3, p. 5). Philadelphia: Saunders.

Parajuli, A., Gautam, A. P., Sharma, S. P., Bhujel, K. B., Sharma, G., Thapa, P. B., ... & Poudel, S. (2020). Forest fire risk mapping using GIS and remote sensing in two major landscapes of Nepal. *Geomatics, Natural Hazards and Risk*, *11*(1), 2569-2586.

Pham, B. T., Jaafari, A., Avand, M., Al-Ansari, N., Dinh Du, T., Yen, H. P. H., ... & Tuyen, T. T. (2020). Performance evaluation of machine learning methods for forest fire modeling and prediction. *Symmetry*, *12*(6), 1022.

Ricotta, C., Bajocco, S., Guglietta, D., & Conedera, M. (2018). Assessing the influence of roads on fire ignition: does land cover matter?. *Fire*, *1*(2), 24.

Saaty, T. L. (1980). Analytic Hierarchy Process Planning, Priority Setting, Resource Allocation. Advanced Optimization and Decision-Making Techniques in Textile Manufacturing, 287.

Saloum, J., & Abdou, H. (2016). Statistical Modeling For Conservation The Vegetation Of The Land In Al Kadmous Area From Rainfall Erosion. *Tishreen University Journal-Arts and Humanities Sciences Series*, *38*(3).

Tiwari, A., Shoab, M., & Dixit, A. (2021). GIS-based forest fire susceptibility modeling in Pauri Garhwal, India: a comparative assessment of frequency ratio, analytic hierarchy process and fuzzy modeling techniques. *Natural hazards*, *105*, 1189-1230.

Vallejo-Villalta, I., Rodríguez-Navas, E., & Márquez-Pérez, J. (2019). Mapping forest fire risk at a local scale—a case study in Andalusia (Spain). *Environments*, *6*(3), 30.

Zhang, K., Shalehy, M. H., Ezaz, G. T., Chakraborty, A., Mohib, K. M., & Liu, L. (2022). An integrated flood risk assessment approach based on coupled hydrological-hydraulic modeling and bottom-up hazard vulnerability analysis. *Environmental Modelling & Software*, *148*, 105279.